Clim. Past, 5, 183–202, 2009
www.clim-past.net/5/183/2009/

Climate of the Past

Impacts of land surface properties and atmospheric CO_2 on the Last Glacial Maximum climate: a factor separation analysis

A.-J. Henrot[1], **L. François**[2], **S. Brewer**[2,*], **and G. Munhoven**[1]

[1]Laboratory of Atmospheric and Planetary Physics, University of Liège, Liège, Belgium
[2]Unité de Modélisation du Climat et des Cycles Biogéochimiques, University of Liège, Liège, Belgium
[*]now at: Botany Department, University of Wyoming, Laramie, Wyoming, USA

Received: 29 October 2008 – Published in Clim. Past Discuss.: 8 January 2009
Revised: 5 May 2009 – Accepted: 23 May 2009 – Published: 3 June 2009

Abstract. Many sensitivity studies have been carried out, using climate models of different degrees of complexity to test the climate response to Last Glacial Maximum boundary conditions. Here, instead of adding the forcings successively as in most previous studies, we applied the separation method of U. Stein et P. Alpert 1993, in order to determine rigorously the different contributions of the boundary condition modifications, and isolate the pure contributions from the interactions among the forcings. We carried out a series of sensitivity experiments with the model of intermediate complexity Planet Simulator, investigating the contributions of the ice sheet expansion and elevation, the lowering of the atmospheric CO_2 and of the vegetation cover change on the LGM climate.

The separation of the ice cover and orographic contributions shows that the ice albedo effect is the main contributor to the cooling of the Northern Hemisphere, whereas orography has only a local cooling impact over the ice sheets. The expansion of ice cover in the Northern Hemisphere causes a disruption of the tropical precipitation, and a southward shift of the ITCZ. The orographic forcing mainly contributes to the disruption of the atmospheric circulation in the Northern Hemisphere, leading to a redistribution of the precipitation, but weakly impacts the tropics. The isolated vegetation contribution also induces strong cooling over the continents of the Northern Hemisphere that further affects the tropical precipitation and reinforce the southward shift of the ITCZ, when combined with the ice forcing. The combinations of the forcings generate many non-linear interactions that reinforce or weaken the pure contributions, depending on the climatic mechanism involved, but they are generally weaker than the pure contributions. Finally, the comparison between the LGM simulated climate and climatic reconstructions over Eurasia suggests that our results reproduce well the southwest to north-east temperature gradients over Eurasia.

Correspondence to: A.-J. Henrot
(alexandra.henrot@ulg.ac.be)

1 Introduction

The Last Glacial Maximum (LGM), around 21 000 years before present (21 kBP), represents the largest climate change of the recent past. It is characterized by an expansion and a thickening of the ice sheets at high latitudes, a large reduction in atmospheric CO_2 concentration and a less dense vegetation cover. Several projects, using palaeoclimatic data, have reconstructed the surface conditions at the LGM, like CLIMAP (CLIMAP Project Members, 1976), or more recently MARGO (Kucera et al., 2005), making the LGM one of the best documented periods of the recent geological past.

As a result, the LGM has become the subject of numerous General Circulation Model (GCM) studies, in order to test the ability of the models to simulate a climate markedly different from the present, and to better understand the mechanisms that lead to abrupt climate changes. Many sensitivity studies have been carried out, using GCMs to test the climate response to various glacial boundary conditions (Broccoli and Manabe, 1987b; Hewitt and Mitchell, 1997; Ganopolski, 2003; Schneider von Deimling et al., 2006).

In these studies, boundary condition changes and forcings were generally applied in a sequential procedure that consisted of a successive addition of the forcings leading to the final LGM state. In that case, the response of the model to a particular change in a given boundary condition is determined by the comparison of the runs with and without that change, neglecting in the analysis the possible interactions

between the forcings that can take place and contribute to the final climate state. To overcome this shortcoming, Stein and Alpert (1993) developed a rigorous method to carry out sensitivity studies that separates the pure contributions of the forcings from the interactions resulting from their combination.

Berger et al. (1996) and Jahn et al. (2005) used the Stein and Alpert (1993) factor separation method to analyse different contributions to the LGM climate. Berger et al. (1996) used a 1-D radiative-convective climate model to assess the individual and synergistic effects of the ice sheet albedo feedback and atmospheric CO_2 changes at LGM. Jahn et al. (2005) used CLIMBER-2 (Petoukhov et al., 2000; Ganopolski et al., 2001) to separate the pure contributions of CO_2, ice sheet and vegetation changes from their combinations. Here, we applied the Stein and Alpert (1993) method to a LGM sensitivity study carried out with the Earth system model Planet Simulator. We carried out a series of sixteen simulation experiments, where we have assessed the effects from differences in the vegetation cover, the ice sheet cover, the orography, and the effect of reduced atmospheric carbon dioxide between a pre-industrial state and the LGM. We reconstructed the vegetation distributions with the CARAIB dynamic vegetation model (described in Sect. 2). We then examined the response of surface temperature and precipitation to the different forcings and discuss the pure contribution of the four factors on the LGM climate, as well as the interactions among them. Finally, we evaluated our LGM results over Eurasia and Africa against LGM climate reconstruction produced by Wu et al. (2007).

2 Model setup

The Planet Simulator (Fraedrich et al., 2005) is an Earth system Model of Intermediate Complexity (EMIC). Its central component is PUMA-2, a spectral GCM with triangular truncation, based upon PUMA (Fraedrich et al., 1998). PUMA-2 solves the moist primitive equations, representing the conservation of momentum, mass and energy, on σ coordinates in the vertical. It also includes boundary layer, precipitation, interactive clouds and radiation parametrizations. For the present study, we configured it to use a T21 truncation and ten vertical equally spaced σ levels. The atmospheric module is coupled to a 50 m deep mixed-layer ocean, a thermodynamic sea-ice and a land surface and soil model. Sea surface temperatures are computed from the net atmospheric heat flux in the surface. The transport of heat by oceanic surface currents is represented by an additional source or sink of heat, varying monthly and spatially that is prescribed within the mixed-layer and the sea-ice. Heat flux adjustments are applied to ocean grid-cells to mimick heat transport by ocean currents that is not an explicitly represented process in the model. Their distribution was determined from a preindustrial experiment, where sea surface temperature and sea-ice distributions were prescribed from the AMIP2 dataset (AMIP2, 2004). This preindustrial heat flux distribution has been used througout the full set of experiments. We did not consider any change in the oceanic circulation at the LGM. The land surface and soil models calculate the surface temperatures from a linearized energy balance equation and predict soil moisture on the basis of a simple bucket model. The influence of vegetation is represented by background albedo and roughness length. Their annual distributions are prescribed, and albedo may only change in grid-cells where snow is present.

The distributions of surface albedo and roughness length were obtained from the dynamic vegetation model CARAIB (CARbon Assimilation In the Biosphere) (Warnant et al., 1994; Nemry et al., 1996; Laurent et al., 2008). CARAIB calculates the carbon fluxes between the atmosphere and the terrestrial biosphere and deduces the evolution of carbon pools, together with the relative abundances of a series of plant types. Its different modules respectively focus on the hydrological cycle, photosynthesis and stomatal regulation, carbon allocation and biomass growth, heterotrophic respiration and litter and soil carbon, and the distribution of the model plant types, as a function of productivity. Here we used a classification with fifteen Plant Functional Types (PFTs), described in Galy et al. (2008). Model derived PFT assemblages were then translated into biomes to produce vegetation maps. The inputs of the model are meteorological variables, which can be taken from meteorological databases or outputs from GCMs. CARAIB has been used before to produce LGM vegetation distributions, using climatic forcings derived from a range of GCM simulation experiments (François et al., 1998, 1999; Otto et al., 2002; Cheddadi et al., 2006; Galy et al., 2008). For the present study, we have derived a new global LGM vegetation distribution, which we discuss in Sect. 4.1.

3 Experimental setup

We carried out a series of sensitivity experiments with the Planet Simulator, implementing the factor separation method of Stein and Alpert (1993). This approach calculates and isolates the pure contribution of any factor, as well as the contributions due to interactions among two or more factors, using a linear combination of a number of simulations. 2^n simulations are then required to separate the pure and interaction contributions of n factors. Following the factor separation method, we carried out a series of sixteen sensitivity experiments, considering all the possible perturbations of a given control run configuration by prescribing changes of ice sheet cover, orography, vegetation cover (through albedo and roughness length) and atmospheric carbon dioxide. Table 1 lists the changes in boundary conditions used for the sixteen experiments. The control experiment (CTRL) does not consider any of the changes, while the LGM experiment

Table 1. Characteristics of the 16 simulation experiments. − refers to control values and + refers to LGM values. Each of the 4 columns corresponds to one of the four factors analysed: atmospheric CO_2, ice cover, orography and surface albedo.

Acronym	CO_2	ICE	ORO	VEG
CTRL	−	−	−	−
C	+	−	−	−
I	−	+	−	−
O	−	−	+	−
V	−	−	−	+
CI	+	+	−	−
CO	+	−	+	−
CV	+	−	−	+
IO	−	+	+	−
IV	−	+	−	+
OV	−	−	+	+
CIO	+	+	+	−
CIV	+	+	−	+
COV	+	−	+	+
IOV	−	+	+	+
LGM	+	+	+	+

includes all of them. We included the LGM land-sea distribution and orbital forcing in the control configuration, taking into account their contributions to produce a complete LGM climate at the end of the series, but neglecting the contribution of their interactions with the other factors, since they are comparatively weak (Sect. 4.2).

A more complete study would have to further consider the effects of ocean circulation changes on the LGM climate. The simple mixed-layer model included in the Planet Simulator precludes the interactive calculation of such circulation changes that would thus have to be prescribed in a similar fashion to the land surface property changes, which we focus on in this study. An adequate prescribed sea surface temperature (SST) distribution, such as those provided by CLIMAP (CLIMAP Project Members, 1976) or MARGO (Kucera et al., 2005) reconstructions, would implicitly take into account such a change. However, there are two main reasons for *not* adopting this approach. First of all, Braconnot et al. (2007) show the limitation of the use of CLIMAP SSTs with slab models, since they fail to produce the magnitude of the glacial cooling, especially in the tropics. Secondly, the use of fixed SSTs constrains the model sensitivity that reduces notably the impacts of vegetation changes outside of land areas (Ganopolski et al., 2001).

Alternatively, we could have derived a LGM heat flux distribution from a coupled ocean-atmosphere or a forced oceanic GCM simulation experiment. However, these simulation experiments do not yet provide a consistent picture on how the ocean circulation changed at the LGM (Weber et al., 2007; Lynch-Stieglitz et al., 2007). Weber et al. (2007) analysed the results from nine different coupled PMIP model simulations. They find that the Atlantic Meridional Overturning Circulation was 10–40% more intense at the LGM than at present-day in four out of nine models, 20–40% less intense in four other models, and slightly reduced only in one model.

We therefore decided to follow the PMIP1 protocol and we prescibed the present-day (control run) oceanic heat flux distributions even for the LGM. As a consequence, the model may respond with a larger sensitivity and simulate cooling closer to coupled ocean-atmosphere ones, if compared to fixed SSTs runs (Braconnot et al., 2007). We must nevertheless keep in mind that some feedbacks and regional impacts of oceanic circulation changes at the LGM (as shown, e.g. by Hewitt et al., 2003 or Kim et al., 2003) cannot be represented.

3.1 Boundary conditions and model configuration

All of the experiments, including the CTRL run, use common orbital forcings, land-sea distribution and oceanic configuration. The orbital parameters correspond to 21 kBP (excentricity 0.018994°, longitude of perihelion 114.42° and obliquity 22.949°). The solar constant is kept fixed at 1365 W/m^2. The model's land distribution takes into account the emergence of land points due to the lower sea-level at 21 kBP. The land-sea mask used with the model has been derived from Peltier's ICE-5G 1° by 1° resolution ice sheet reconstruction (Peltier, 2004), interpolated onto the model's grid.

In order to have a common land-sea mask for all of the sixteen simulation experiments, the CTRL run already takes into account the exposure of land at the LGM that results from ice sheet growth. We chose not to include this land-sea mask change in the orography changes, since it brings about additional changes, such as vegetation cover or ice cover, which are analysed separately. Therefore, the effect of orography changes on the LGM climate considered here only relates to the increase of elevation at high latitudes. The emerging cells from the LGM land-sea distribution therefore also kept their oceanic albedo and roughness length in the CTRL run, making it as similar as possible to a pre-industrial configuration.

As initial conditions over ocean gridpoints, we used the preindustrial SST and sea-ice distributions. The boundary conditions in time are given by the heat transfer calculated by the Planet Simulator for a preindustrial climate, following the PMIP1 protocol.

The CTRL experiment used a preindustrial atmospheric CO_2 concentration of 280 ppmv. The control continental ice cover and orography have also been reconstructed from Peltier's ICE-5G for the preindustrial state, considering that grid-cells covered by an ice fraction greater than 50% are completely covered by ice (see Fig. 1). The vegetation parameters have been derived from a preindustrial vegetation distribution calculated from an equilibrium run of CARAIB, forced with 280 ppmv of CO_2 and the climatology of the

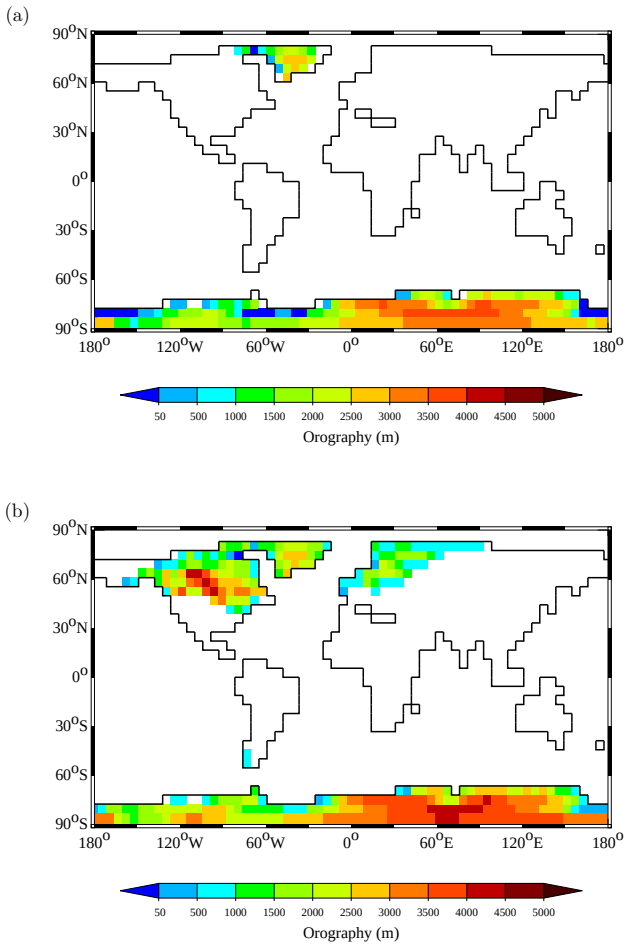

Fig. 1. Land-sea mask and orography over the glacier mask for **(a)** the CTRL configuration and **(b)** the LGM configuration. The ice sheet expansion is shown by the colored pixels.

CLIMATE database version 2.1 (W. Cramer, Potsdam, personal communication).

To obtain the LGM climate, we lowered the atmospheric CO_2 concentration to an ice age level of 200 ppmv (Petit et al., 1999). We reconstructed the continental ice cover and orography from Peltier's ICE-5G for the LGM (see Fig. 1). The vegetation parameters have been replaced by their LGM distributions derived from a LGM vegetation distribution produced by CARAIB, except over the land points that are covered by ice sheets at LGM, in order to not overestimate the vegetation impact. We used an equilibrium run of CARAIB forced with 200 ppmv of CO_2 and a climate derived from the ECHAM4 GCM (Roeckner et al., 1996) (revised version of the distribution shown by François et al. (2003)). We calculated the anomalies of the GCM climatic fields between the LGM and the preindustrial, added to the CLIMATE database version 2.1, as climatic inputs for the LGM simulation, following the approach described in Otto et al. (2002).

Neither the effects of lower CH_4 and N_2O concentrations in the atmosphere, nor those of the higher atmospheric dust content at the LGM have been taken into account here. These three agents are not included in the radiation scheme of the Planet Simulator. Their variations could lead to important additional cooling and provide feedbacks for the LGM climate system. This is well documented by the results of Schneider von Deimling et al. (2006) who show that the increase of atmospheric dust at the LGM yields a net global cooling that is of the same order of magnitude than the vegetation induced cooling.

4 Results

4.1 Simulated LGM vegetation

The biome maps (Fig. 2) show the simulated preindustrial and LGM vegetation distributions, with a resolution of 0.5° by 0.5°. Globally, the simulated LGM vegetation cover is less dense than the preindustrial one. Grasslands and deserts expand, mainly at the expense of forest ecosystems, in response to the extremely cold and dry LGM conditions. CARAIB simulates a reduction of the total carbon stock (vegetation plus soil) of 734 Gt C, which is at the lower end of the LGM carbon stock reduction range suggested from reconstructions of palaeovegetation from palynological and sedimentological proxy data (−700 to −1600 Gt C), but slightly higher than estimates obtained with biospheric model forced with outputs of general circulation models (0 to 700 Gt C, after Pedersen et al., 2003).

Regionally, the simulated LGM vegetation distribution is broadly consistent with the results of the Palaeovegetation Mapping Project BIOME 6000[1] (Prentice and Jolly, 2000; Harrison et al., 2001; Bigelow et al., 2003; Pickett et al., 2004). Polar desert and tundra are modelled in a large part of the Northern Hemisphere continents. In Siberia and in the part of Alaska not covered by ice sheets, they replace the boreal forests (taïga), when in Western Europe tundra replaces the temperate forests. Note that the polar desert or ice biome, extremely expanded in our LGM simulation, does not represent permanent ice, but the absence of vegetation, due to extremely cold and dry conditions. The warm temperate and mixed forests of Southwestern Europe are replaced by semi-deserts. Colder forest types also appear in our results, as in the reconstruction of Cheddadi et al. (2006). This latter reconstruction differs from the BIOME 6000 one and shows only semi-deserts in the region. North Africa is covered by deserts, with a southward expansion of the Sahara by less than 5° in latitude, replacing tropical grasslands or savannas. In Equatorial Africa the tropical rainforest is reduced, except in the western part. In Asia, deserts and grasslands expand, with an extension of deserts to the east in the center of Asia,

[1] available under http://www.bridge.bris.ac.uk/resources/Databases/BIOMES_data

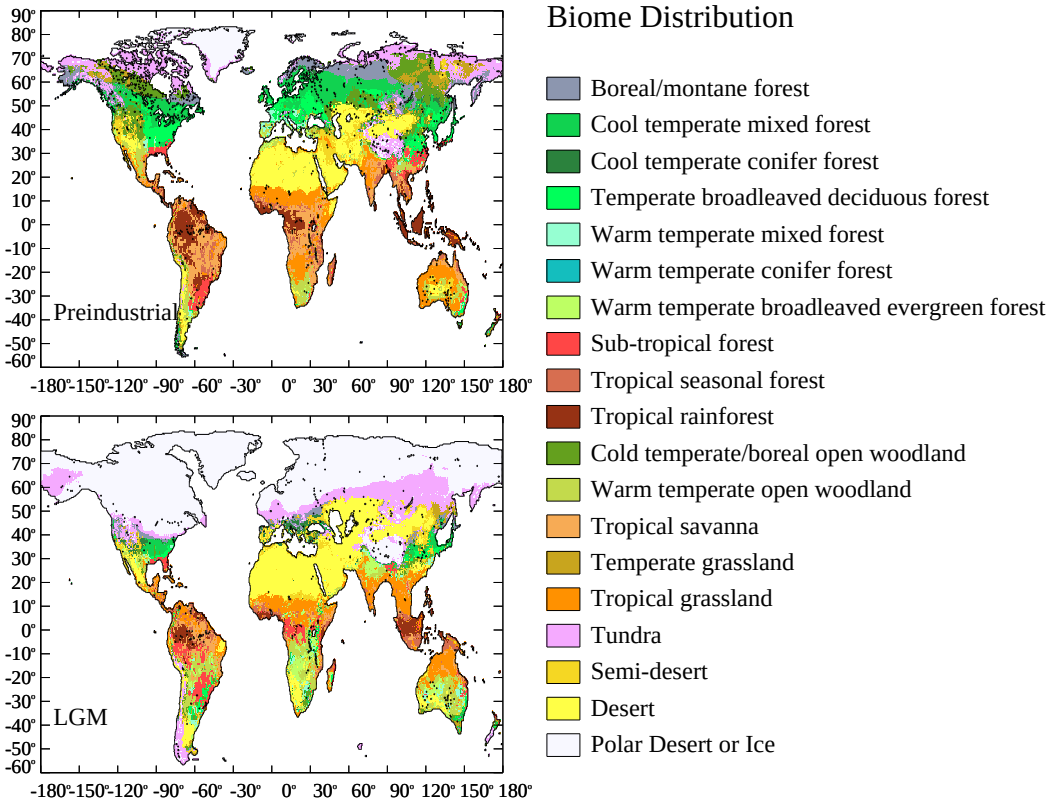

Fig. 2. Biome distributions from CARAIB preindustrial and LGM equilibrium runs.

and the replacement of subtropical and temperate forests by tropical grasslands essentially in Southeastern Asia. In North America, the forest biomes are shifted southwards and replaced by tundra or polar deserts, and the subtropical types are limited to Florida. However, the predominance of deserts and grasslands in the west coast of North America, simulated by CARAIB, does not agree with the reconstructions of Williams et al. (2000) used in the BIOME6000 results, which show mainly cool mixed forests and open woodlands in this region. It is more in line with the recontruction of Adams et al. (1990). A fragmentation of the tropical rainforest and its remplacement by savannas or subtropical forests occur in the north of South America, while the southern part is dominated by tundra and deserts. Finally, the tropical grasslands and deserts prevailing in the center and the southwest of Australia in the simulated preindustrial distribution are replaced by warm and open forests.

4.2 Control experiment

As mentioned before, the control state differs from a preindustrial one by the 21 kBP orbital configuration and land-sea distribution that we separate from the other factors, due to the weak contributions of their interactions. Nevertheless, the pure effects of both factors contribute to the LGM climate. The change in the orbital forcing reduces the global mean surface temperature by 0.4°C from 15.2°C at preindustrial times, but it does not significantly affect the precipitation. Local cooling does not exceed −0.5°C over the continents and the open ocean. It may nevertheless reach −4°C over sea-ice, especially in the Antarctic ocean, due to the persistence of sea-ice in summer, following the lowering of the obliquity at 21 kBP that reduces insolation at high latitudes in both hemispheres during their respective summers. The modification of the land-sea mask (with emerging grid-cells keeping oceanic surface albedo) warms the global mean temperature by 0.3°C. This warming is mainly due to the replacement of ocean by land grid-cells, preventing the formation of sea-ice on some grid-cells at high latitudes and the resulting strong albedo feedback to take place, and limiting the evaporation on some emerged grid-cells in the tropics. Finally, the CTRL climate, combining both forcings, is close to a preindustrial climate (with a global surface temperature lowered by −0.1°C only). The surface temperature and precipitation distributions for the control state are shown on Fig. 3.

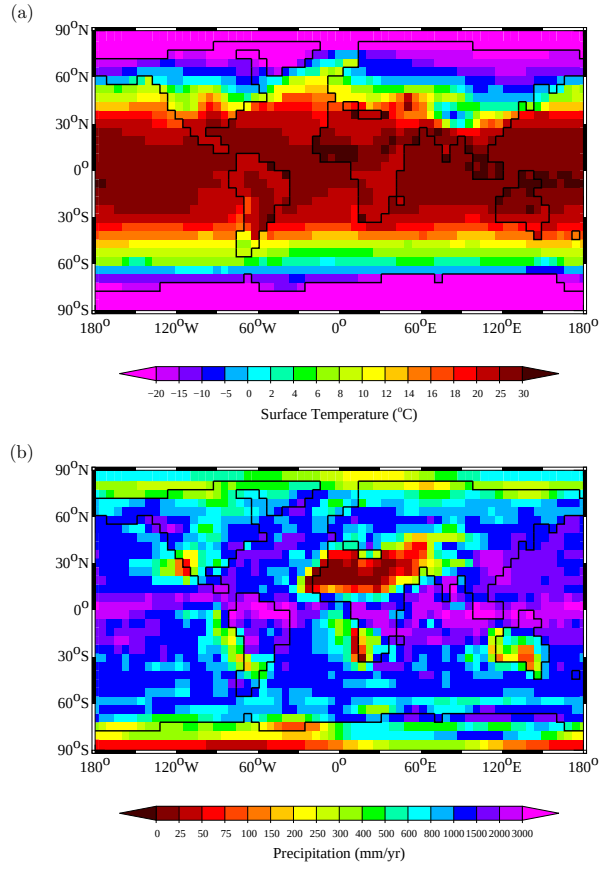

Fig. 3. Control experiment (CTRL) results: **(a)** annual surface temperature; **(b)** precipitation.

4.3 Global responses

We present here the global impacts of the pure contributions of the four factors, as well as the contributions of their interactions. The magnitude of the impacts of boundary condition changes on surface temperature and precipitation are shown in Fig. 4, representing the anomalies between each experiment and the control run. Ice cover change (experiment I) is the factor producing globally the largest cooling and dryness, followed by CO_2 (experiment C) that gives an additional cooling effect when added to the ice cover change (experiment CI). Vegetation cover changes also significantly cool and dry the climate (experiment V), when orography changes slightly tend to warm the global climate (experiment O). The experiment CIV, adding ice, CO_2 and vegetation changes, is then the coolest and the dryest of the series, even more than the complete LGM one, due to the absence of orography change. The global LGM cooling is -5.2°C (-10.4°C on the continents and -1.8°C on the oceans), and the global LGM precipitation reduction is -79 mm/yr (-105 mm/yr on the continents and -45 mm/yr on the oceans).

Table 2. Comparison of the pure contributions with the effects of the interactions between the factors on the global, oceanic and continental annual surface temperature (in °C). (See Fig. 5 for additional information.)

Acronym	Global	Ocean	Continent
C	−2	−1.9	−1.9
I	−2.7	−1.4	−5.7
O	+0.1	+0.4	−0.9
V	−1.3	−0.8	−2.5
CI	+0.1	+0.0	+0.1
CO	+0.1	+0.1	+0.1
CV	−0.0	−0.1	+0.2
IO	+0.2	+0.1	+0.4
IV	+0.2	+0.1	+0.5
OV	+0.1	+0.1	+0.0
CIO	+0.1	+0.1	−0.1
CIV	+0.1	+0.2	−0.2
COV	+0.0	+0.2	−0.3
IOV	+0.0	+0.1	−0.1
LGM	−0.0	−0.1	+0.1

Table 3. Comparison of the pure contributions with the effects of the interactions between the factors on the global, oceanic and continental annual precipitation (in mm/yr). (See Fig. 5 for additional information.)

Acronym	Global	Ocean	Continent
C	−33	−29	−33
I	−47	−23	−99
O	−1	−2	−1
V	−29	−5	−77
CI	+4	+4	+5
CO	+0	−4	+9
CV	+2	−0	+8
IO	+5	+4	+7
IV	+13	+5	+31
OV	+2	−1	+6
CIO	+1	+6	−9
CIV	+2	−0	+6
COV	+2	+5	−4
IOV	+1	+4	−3
LGM	−4	−8	−0

The LGM cooling obtained here is consistent with the cooling simulated by the models used in PMIP1 (from -2 to -6°C for atmospheric GCMs with computed sea surface temperatures (Joussaume and Taylor, 2000)) and PMIP2 (between -3.6 and -5.7°C for coupled atmosphere-ocean models (Braconnot et al., 2007)), but it is at the cooler end of this range. This may be due to the lack of an explicit representation of ocean circulation in our model, as the slab models used in PMIP1 tended to produce stronger cooling over the Northern Hemisphere than the coupled

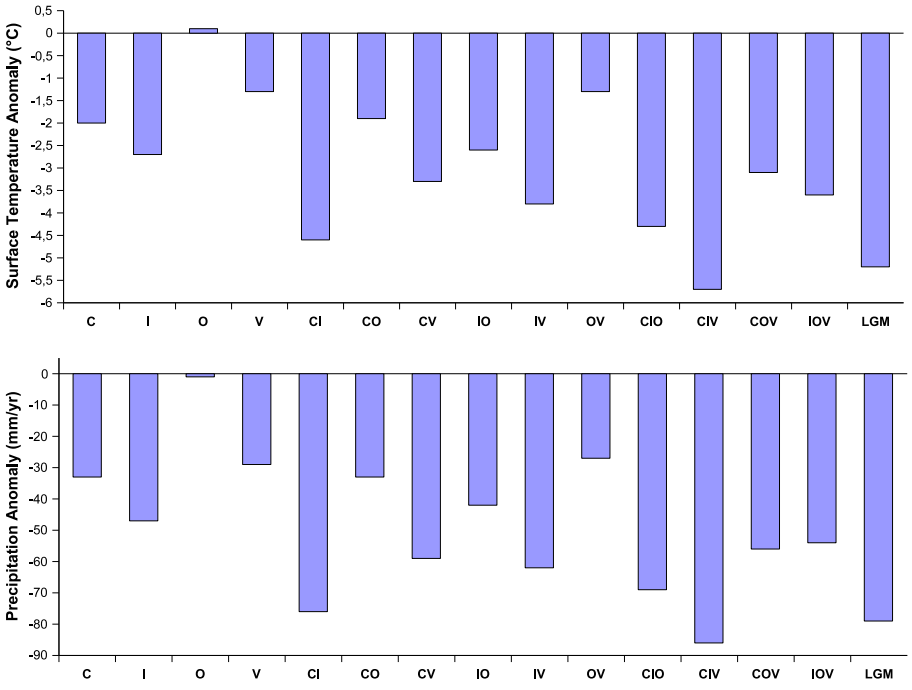

Fig. 4. Global surface temperature and precipitation anomalies (EXPERIMENT-minus-CTRL). All results reported here are global means over the last 20 years of 50-year simulations, allowing 30 years for the model to equilibrate.

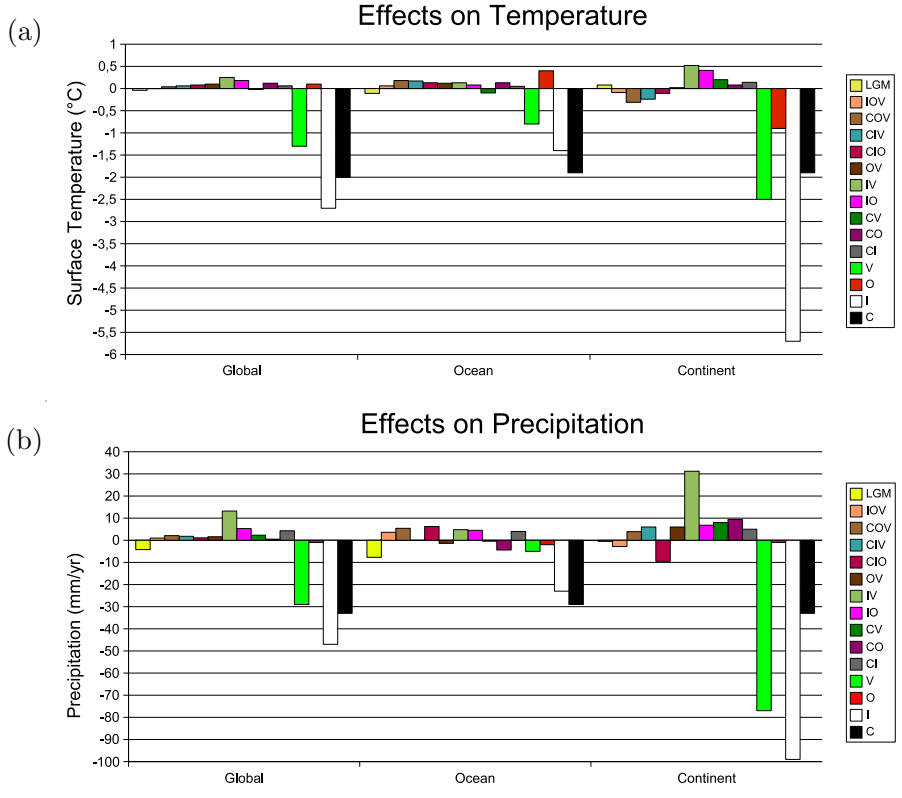

Fig. 5. Comparison of the pure contributions with the effects of the interactions between the factors on the global, oceanic and continental annual **(a)** surface temperature and **(b)** precipitation. The C, I, O, V effects represent the pure contributions of each factor. The CI to LGM effects represent the contributions of the *interactions* among the corresponding factors, not the actual effects, shown on Fig. 4.

ocean-atmosphere models (Braconnot et al., 2007). However, none of the PMIP1 models and only a few of the PMIP2 models have taken into account vegetation changes at LGM. The additional cooling simulated in our experiments may therefore be also due to the additional contribution of vegetation change. This is partially supported by the CIO experiment, which does not include vegetation changes. This simulated a global temperature anomaly of -4.3°C, which better fits the range of the PMIP1 and PMIP2 model cooling than the total LGM cooling of -5.2°C.

The impacts of the interactions of two or more factors on global, continental and oceanic surface temperature are shown respectively on Fig. 5a and Table 2, and on Fig. 5b and Table 3. The contributions of the pure factors (ice, CO_2, vegetation and orography anomalies) are also shown for comparison. Note that we do not consider Antarctica in the calculation of the continental mean. Large changes especially in surface temperature that have only a weak impact on local climate and are not indicative of large scale climate change, can occur there. The interactions should be taken into account in the climate analysis, since they show evidence of the non linear feature of effects caused by the different factor combinations. For example, the combination of the ice and vegetation cover changes (experiment IV) produces non linear effects that result in an increase of surface temperature and precipitation. These effects act in the opposite direction of the pure contributions of ice and vegetation. The total cooling due to ice and vegetation cover changes (-3.8°C on global surface temperature, see Fig. 4) is then weaker than the simple addition of both pure contributions (-2.7°C for ice plus -1.3°C for vegetation that is -4°C), since the interaction between both forcings gives a slight warming (of $+0.2$°C globally). Nevertheless, the interaction effects remain weaker than the pure contributions effects. Only the interactions between ice and vegetation, and ice and orography (experiments IV and IO) have comparable effects to the pure contribution ones, especially on the continents. The interaction IO notably warms the continental surface temperature by 0.4 °C, while the pure orographic contribution leads to a continental warming of 0.9°C (Fig. 5). The increase of precipitation caused by the interaction IV ($+31$ mm/yr) also compares to the decrease of precipitation due to the CO_2 contribution (-33 mm/yr) (Fig. 5).

4.4 Spatial responses

4.4.1 Surface temperature

Figures 6 and 7 illustrate the surface temperature responses to the prescription of the boundary condition forcings. The presence of ice sheets increases the albedo of ice covered grid-cells by more than 40% in comparison to the control state. The pure ice cover effect (experiment I, Fig. 6a) produces the largest cooling only in the Northern Hemisphere, in comparison to the other pure contributions of the series, but weakly affects the Southern Hemisphere. The weak impact of the ice cover effect in the Southern Hemisphere is due to the lack of ocanic circulation changes in our model. Only the small ice cap covering Patagonia leads to a pronounced local cooling. The largest decreases of surface temperature are located over the ice sheets and over the North Atlantic and the Arctic Oceans, resulting from an extension and thickening of sea-ice. The mid and low northern latitudes are also affected by some weaker cooling, but some tropical regions, as Equatorial Africa and India, are subjected to warming that is more pronounced during summer and linked to a decrease of summer rainfall.

Vegetation cover changes result in a large cooling on the Northern Hemisphere, mainly over the continents (experiment V, Fig. 6c). The vegetation contribution is comparable in terms of magnitude to the ice cover effect over the mid and low latitudes of the Northern Hemisphere. As described above, vegetation cover changes affect surface albedo and roughness length, but the albedo impact on surface temperature is dominant, because of its direct impact on the energy balance. The cooling produced on the continents of the Northern Hemisphere is directly linked to the increase of surface albedo by more than 10%, caused by the replacement of boreal and temperate forests by tundra or semi-deserts. Further, the induced cooling can be reinforced by the snow albedo feedback, on grid-cells covered by snow. However, Equatorial Africa and India also show some warming, related to a decrease of evaporation and summer rainfall, as in experiment I. Surface temperatures also increase in Australia and South Africa, but are caused instead by the increase of surface albedo, caused by the replacement of deserts and grasslands by forest biomes. Finally, there is pronounced but localized cooling over emerging land grid-cells at LGM, due to the replacement of their control oceanic albedos of 7% directly by LGM vegetation albedo greater than 15%. In experiment IV (Fig. 7a), the application of vegetation changes together with the presence of ice sheets reinforces and expands southwards the cooling induced by the ice cover effect, especially over the high latitudes and the continents in the Northern Hemisphere. A stronger warming occurs in Equatorial Africa and India. However, the Southern Hemisphere remains weakly affected by both factors. Only vegetation changes produce a weak warming, due to a decrease in albedo.

The CO_2 contribution causes a rather uniform temperature cooling, of about –2°C (experiment C, Fig. 6d). The magnitude of the cooling is similar over continents and oceans, and in both Northern and Southern Hemispheres, making it the most important contributor to sea surface temperature cooling. Further, the CO_2 contribution results in a stronger cooling around the poles, especially over the Antarctic ocean, linked to an expansion and thickening of sea-ice. This reinforces the cooling trend in the Northern Hemisphere initiated by ice sheet and vegetation albedo effects, when all three forcings are combined (experiment CIV, Fig. 7c), and gives

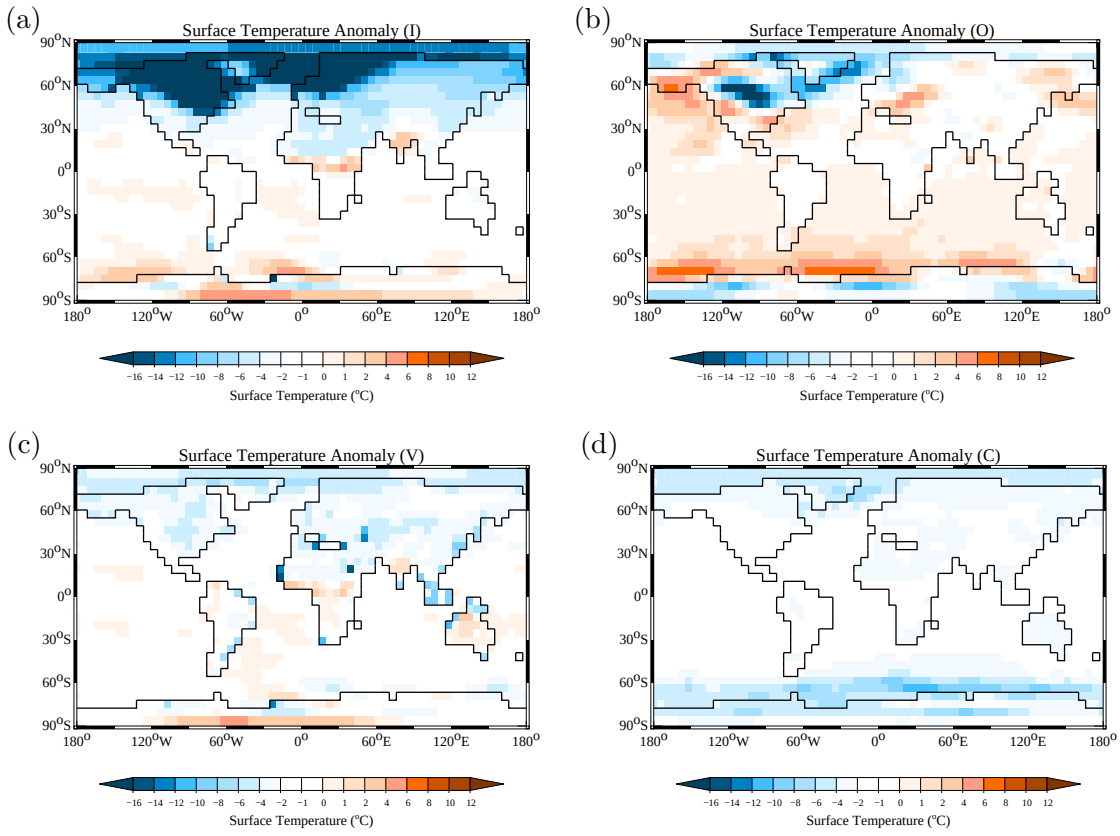

Fig. 6. Annual surface temperature anomalies (EXPERIMENT-minus-CTRL) for **(a)** experiment I; **(b)** experiment O; **(c)** experiment V; **(d)** experiment C.

an additional cooling in the Southern Hemisphere, notably stronger than the vegetation warming impact in Australia and South Africa.

In contrast to the previous contributions, orography changes do not have a net cooling effect in the Northern Hemisphere (experiment O, Fig. 6b). The increased elevation produces large cooling over the ice sheets, especially over the Laurentide ice sheet, which has its surface at 3000 m a.s.l. in the LGM reconstruction. The cooling also affects the Arctic and North Atlantic oceans. However, North America, Europe and also the West Pacific and North Atlantic experience large warming linked to precipitation changes, caused by wind track perturbations at mid and high latitudes, as discussed below. The combination of the ice sheet cover and orography forcings, representing the full contribution of the ice sheets on surface temperature of the ice sheets at LGM, leads to an additional cooling over the ice sheets (Fig. 7b). The cooling is weaker over the southern borders of the ice sheets, due to the orographic contribution. The cooling trend induced by the ice cover remains dominant over the continents of the Northern Hemisphere, whereas the orography changes minimize the cooling at the mid latitudes and slightly warm some oceanic regions, e.g. North West Pacific and Southern Ocean, where the ice albedo has weaker impacts.

The combination of the four factors (experiment LGM, Fig. 7d), keeps the cooling profile induced by ice cover, vegetation and CO_2 changes, as in the experiment CIV. However, experiment LGM is warmer than experiment CIV, due to the contribution of orography changes, warming the oceans and some continental regions of the mid latitudes in the Northern Hemisphere.

4.4.2 Precipitation

Figures 8 and 9 illustrate the significative precipitation responses to the prescribed boundary condition forcings. In experiment I (Fig. 8a), the cooling induced by the ice cover effect dries out the atmosphere, and reduces precipitation. Large reductions occur in the Northern Hemisphere, over the ice sheets, Siberia, Alaska and the North Atlantic Ocean. Further, the intense cooling of the continents strengthens the westerlies of the Northern Hemisphere, giving rise to precipitation in North America and North Pacific. Nevertheless, the impact of ice cover is not limited to the high latitudes and also strongly influences the tropical precipitation system by a southward shift of the control location of the Inter Tropical Convergence Zone (ITCZ). The strong cooling impact of ice cover on the surface and sea surface temperature

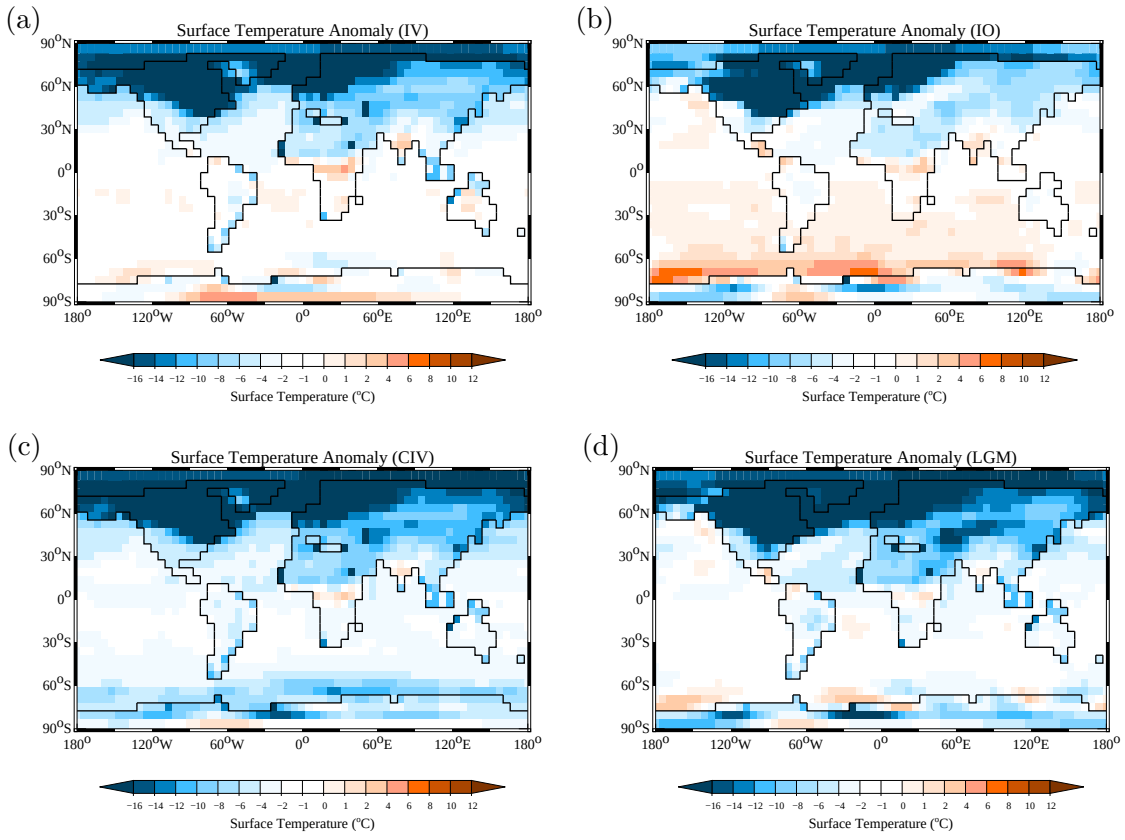

Fig. 7. Annual surface temperature anomalies (EXPERIMENT-minus-CTRL) for **(a)** experiment IV; **(b)** experiment IO; **(c)** experiment CIV; **(d)** experiment LGM.

in the Northern Hemisphere causes an increase of the inter-hemispheric temperature gradient, sufficient to lead to a displacement of the ITCZ to the warmer Southern Hemisphere. This explains the reduction of precipitation over the oceans and the continent and the weakening of the monsoon systems (except over southeastern China) in the northern part of the tropics (ITCZ control location), and the increase of precipitation to the south.

Vegetation changes in experiment V (Fig. 8c) in turn dry out the continents of the Northern Hemisphere, mainly due to the cooling effect of the increase of albedo. The cooling effect again strengthens the westerlies, increasing precipitation over the center of North America, and is similar, but weaker in magnitude, to the ice cover effect. The tropics also undergo a strong reduction of precipitation, as in experiment I. By the same mechanism, the contribution of the vegetation changes is then sufficient to shift the ITCZ location southwards, reducing oceanic and continental precipitation in the northern part of the tropics. Nevertheless, the reduction of the rainforest in Amazonia, Equatorial Africa or Indonesia could also be responsible for the reduction of precipitation over these regions. The change of vegetation from rainforest to grasslands or savannas decreases the roughness length that in turn decreases the surface evaporation, thus warming and drying the air. The change in precipitation could be linked to the roughness length more than to the albedo effect. The combination of vegetation changes with ice cover (Fig. 9a) reinforces the dryness induced by ice albedo in the Northern Hemisphere, and intensifies the ITCZ shift, further decreasing rainfall over the ITCZ control location and increasing them southwards.

Orography changes strongly affect precipitation over the mid and high latitudes of the Northern Hemisphere, by disrupting the atmospheric circulation (Fig. 8b). The presence of the high Laurentide ice sheet causes a split flow of the westerlies into two branches, one passing northwards of the ice sheet and the other southwards, and rejoining over the North Atlantic. As we can see on Fig. 10, showing the surface winter winds for the experiments CTRL and O, the split flow causes at the surface a deflection of the westerlies over Alaska and the formation of an anticyclonic circulation over the western portion of the Laurentide ice sheet. The northern part of the ice sheet is then crossed by a strong surface flow that increases precipitation there, while the southern part and the rest of North America is crossed by north to northwest flow originating from the anticyclone that causes a decrease

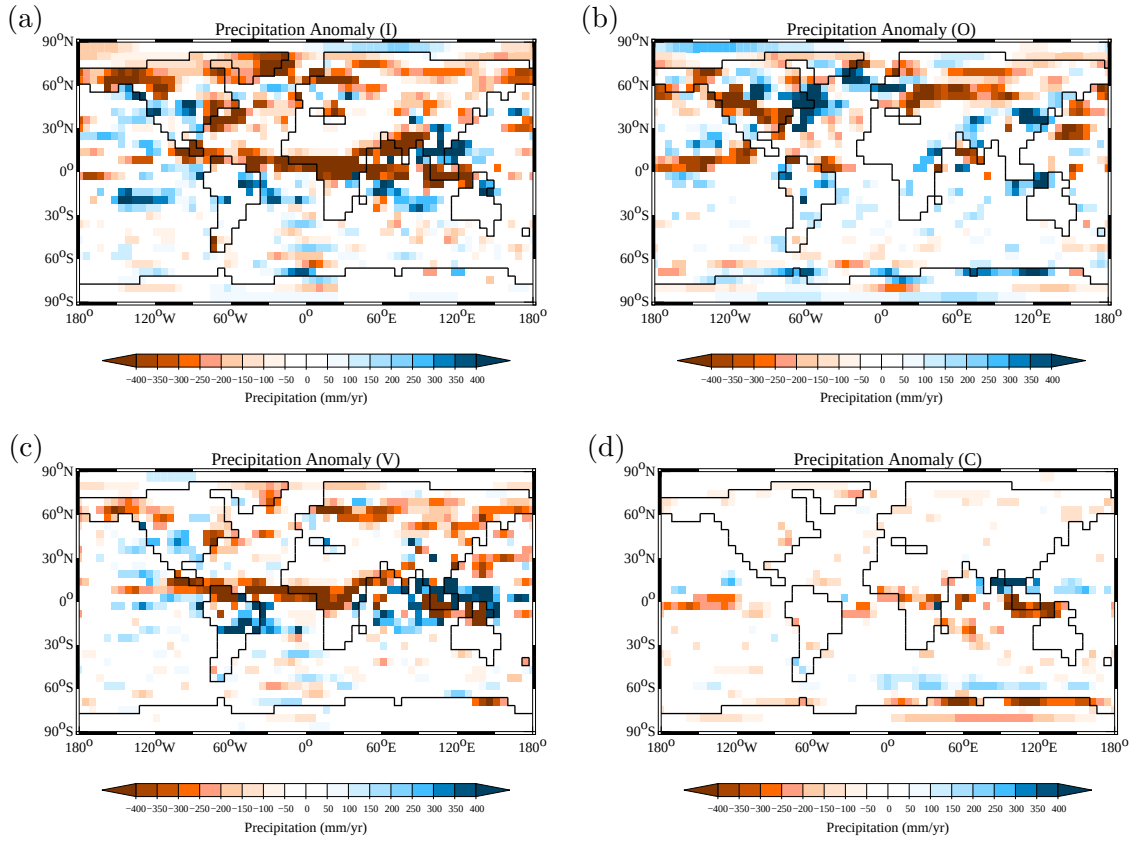

Fig. 8. Annual precipitation anomalies (EXPERIMENT-minus-CTRL) for **(a)** experiment I; **(b)** experiment O; **(c)** experiment V; **(d)** experiment C. Only anomalies greater than one standard deviation for the long-term annual mean over the last 20 simulation years are shown.

of rainfall in these region. These conditions prevail during winter, spring and autumn, but weaken during summer. Over the North Atlantic, where both flows merge together, precipitation generally increases. The deflection of the westerly wind belt over the North Altantic, with south to southwest winds arriving to the southern part of the Fennonscandian ice sheet, increases precipitation on the ocean. However, it decreases the wind strength over Western Europe, causing a large reduction of precipitation in the main part of Eurasia, explaining the net warming of the surface temperature described above. The Fennoscandian ice sheet also blocks the westerlies that contributes to the decrease of precipitation over Eurasia. The total ice sheet contribution, combining ice cover and orography forcings (experiment IO, Fig. 9b), keeps the precipitation profile imposed by orography changes in the Northern Hemisphere, and imposed by the ice albedo in the tropics. Nevertheless, the ice albedo cooling effect tends to increase the dryness of the continents of the Northern Hemisphere, except over North America, where the intensification of the westerlies causes more precipitation. The shift of the ITCZ over the ocean is more pronounced that can be linked to the further increase of the surface temperature gradient, due to warmer sea surface temperatures in the south, induced by orography changes.

The CO_2 contribution has the weakest impact on precipitation in the Northern Hemisphere, and dries out equally both hemispheres (Fig. 8d). Only the equatorial band is affected by a more pronounced decrease of precipitation, still weaker than the other pure contributions that can be related to the CO_2 induced sea surface temperature cooling. The combination of the CO_2 effect with the ice cover and vegetation change effects (Fig. 9c), generates the driest experiment of the series (experiment CIV), causing strong reductions of precipitation over the continents and a pronounced southward shift of the ITCZ. The addition of the orography contribution, in the experiment LGM (Fig. 9d), essentially modifies the precipitation distributions in the Northern Hemisphere, generating more precipitation over the north and north-west of the Laurentide ice sheet, in comparison to the experiment CIV. However, the drying over the continents of the Northern Hemisphere is reinforced, as well as the decrease of rainfall over the ITCZ control location.

4.4.3 Interaction effects

The global effect of the interactions among factors generally tend to increase temperatures and precipitation. However, the interactions have much more contrasted local effects, which

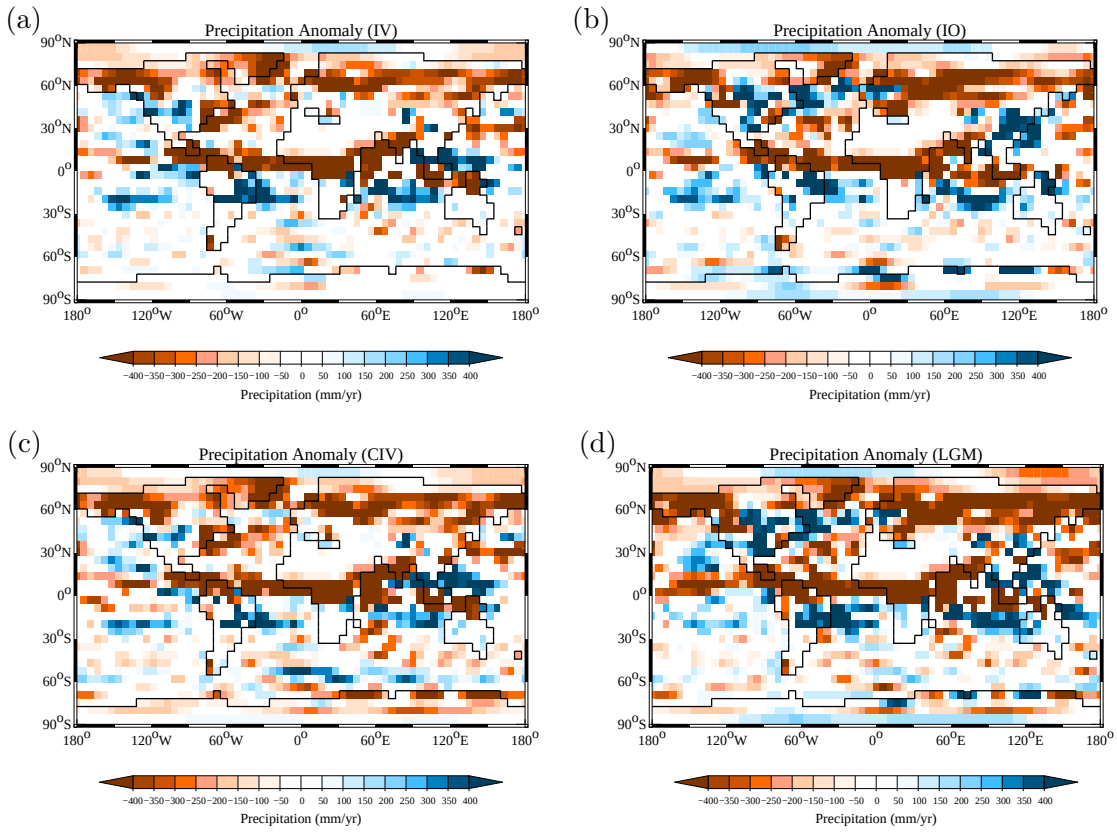

Fig. 9. Annual precipitation anomalies (EXPERIMENT-minus-CTRL) for **(a)** experiment IV; **(b)** experiment IO; **(c)** experiment CIV; **(d)** experiment LGM. Only the anomalies greater than one standard deviation for the long-term annual mean over the last 20 simulation years are shown.

may weaken or reinforce the pure contribution effects, depending on the region. We discuss here only the strongest interactions of the series, which are the interactions between ice cover and vegetation change (IV), and between ice cover and orography changes (IO), respectively. The other interactions of the series (OV, IOV, etc.) show similar patterns in their effects, but are weaker. We can also remark that the interactions between CO_2 changes and the other factors generates the weakest effects of the series. Figure 11 shows the effects on surface temperature and precipitation of the interactions IV and IO.

Both interactions IV and IO warm the surface temperature over sea-ice in the Arctic Ocean, with the interaction IO causing a greater warming, even affecting the northern borders of the continents. The interactions here weaken the pure contributions of the three factors that tend to increase the sea-ice extent and thickness in the Arctic, reducing the regional climate cooling. In contrast, in the Antarctic Ocean, the interactions favor the sea-ice extent and thickening.

The interaction IV produces strong continental cooling, comparable in magnitude to the pure contributions, e.g. in Alaska (Fig. 11a). The increase of surface albedo due to both contributions cools the surface temperature, allowing snow to persist and the positive snow albedo feedback to reinforce the initial cooling induced by both pure contributions. However, over Equatorial Africa and India, the interaction leads to a cooling together with a precipitation increase (Fig. 11c). These effects can be related to a more important surface evaporation, permitted by the decrease of the sensible heat flux, due to the southward extension of the cooling trend caused by both I and V forcings. In this case, the interaction acts in the opposite direction of both pure contributions, and lowers their regional warming impacts.

The interaction IO produces strong cooling over the continents, particularly over North America, with an increase of rainfall (Fig. 11b and d). The interaction effect is opposite to the orographic warming effect in the concerned region. This regional cooling can be related to the ice induced cooling, reinforced by the snow albedo feedback, and possibly to the local topographic cooling induced by the orography change. However, precipitation also increases, related to the combined effects of the strengthening of the winds due to the ice contribution and the intensification of the northern branch of the jet stream due to the orography contribution.

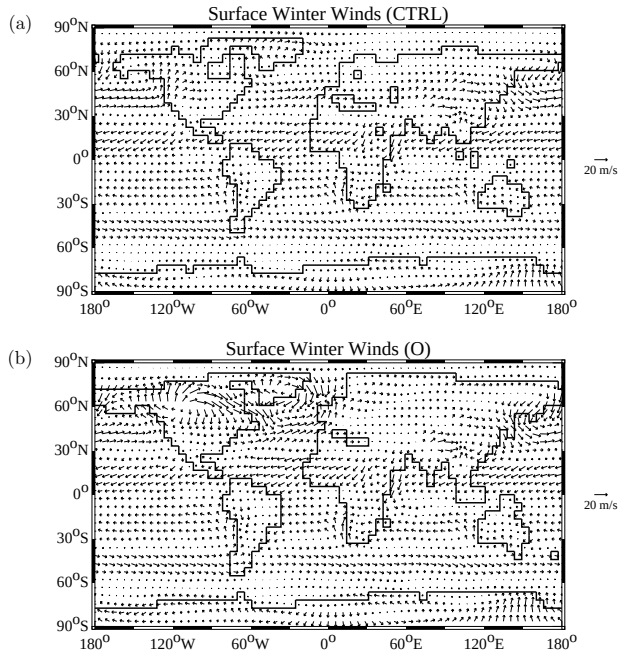

Fig. 10. Surface winter winds resulting for **(a)** experiment CTRL **(b)** experiment O.

However, the interaction IO mainly affects the precipitation in the Northern Hemisphere, while the interaction IV essentially affects the tropics.

5 Discussion

5.1 Effects on surface temperature

The complete series of experiments allows us to analyse and distinguish several climatic impacts on the LGM climate, linked to the development of ice sheets, the lowering of atmospheric CO_2 and vegetation changes. The factor separation method of Stein and Alpert (1993) used here allows us to compare the relative roles of the factors, starting from the same control state. This procedure was previously adopted in the LGM climate studies of Berger et al. (1996) and Jahn et al. (2005). It differs from the sequential procedure used in most previous sensitivity studies on the climate forcings at the LGM (Broccoli and Manabe, 1987b; Hewitt and Mitchell, 1997; Ganopolski, 2003; Schneider von Deimling et al., 2006). The results derived from the sequential additive procedure are particulary sensitive to threshold effects, that could trigger large non-linear changes in the system when crossed. In consequence, the magnitude of a given effect would be dependent on the order in which the forcings are applied. The factor separation method suffers less from this shortcoming. With this method, non-linear climate response is included in the interaction terms that the method allows to isolate from the pure contributions of the factors. Once the joint action of two or more processes makes the system cross a threshold, care needs to be taken to interpret the physical meaning of the interaction terms, as discussed by Jahn et al. (2005). The major disadvantage of the factor separation method is that it requires a large number of experiments to be carried out that can be minimized by a rigorous choice of the forcing studied. It is also best suited for use with EMICs, which allow to keep the required computing time within reasonable bounds.

In the following section, we compare our results to those of Ganopolski (2003) and Jahn et al. (2005), who performed sensitivity studies with the CLIMBER-2 model. Ganopolski (2003) used a sequential additive procedure, Jahn et al. (2005) the factor separation method. We obtain a global LGM cooling of -5.2°C that compares well with the global cooling of -5.1°C obtained by Jahn et al. (2005). The magnitudes of the global contributions show the dominant cooling effect of the ice sheets (combined albedo-temperature and altitude-temperature effects) that is -3°C in Ganopolski (2003) and in Jahn et al. (2005) and -2.6°C in our experiment IO. The reduction of atmospheric CO_2 is the second major factor responsible for cooling the LGM climate globally, as already shown by Broccoli and Manabe (1987b). Reducing the concentration to 200 ppm (Ganopolski, 2003) and to 190 ppm (Jahn et al., 2005) respectively cools the climate by 1.2°C and 1.5°C. Here, the lowering of the concentration to 200 ppm (experiment C) cools the climate by 2°C, due to the high sensitivity of PLASIM to CO_2 (Fraedrich et al., 2005b).

Locally, the presence of ice sheets cools mainly the high latitudes of the Northern Hemisphere in both models. However, due to the lack of oceanic circulation in our model, we do not reproduce the strengthening of the northward oceanic heat transfer that weakens the cooling in the Northern Hemisphere and reinforces the cooling in the Southern Hemisphere (Jahn et al., 2005). This explains the greater cooling produced in the Northern Hemisphere and some warming obtained in the Southern Ocean in experiment IO, in comparison to Jahn et al. (2005).

The lowering of atmospheric CO_2 mainly contributes to the sea-ice formation at high latitudes. In experiment C, it has a homogeneous cooling and drying effect in both hemispheres. Its local contribution, especially on the continents in the Northern Hemisphere, is the weakest of the four pure contributions. In Jahn et al. (2005), the lower CO_2 also impacts on the oceanic circulation, and reinforces once more the heat transfer to the North, leading to a stronger cooling in the Southern Hemisphere, if compared to our experiment C. Further, CO_2 induces in our results very weak non linear interactions with the other factors and always tends to reinforce the cooling and the drying induced by the other factors. Due to the lack of oceanic circulation, we have possibly missed further oceanic feedbacks and their interactions. Jahn et al. (2005) obtained a switch from a warm ocean mode to a cold ocean mode (Ganopolski and Rahmstorf, 2001),

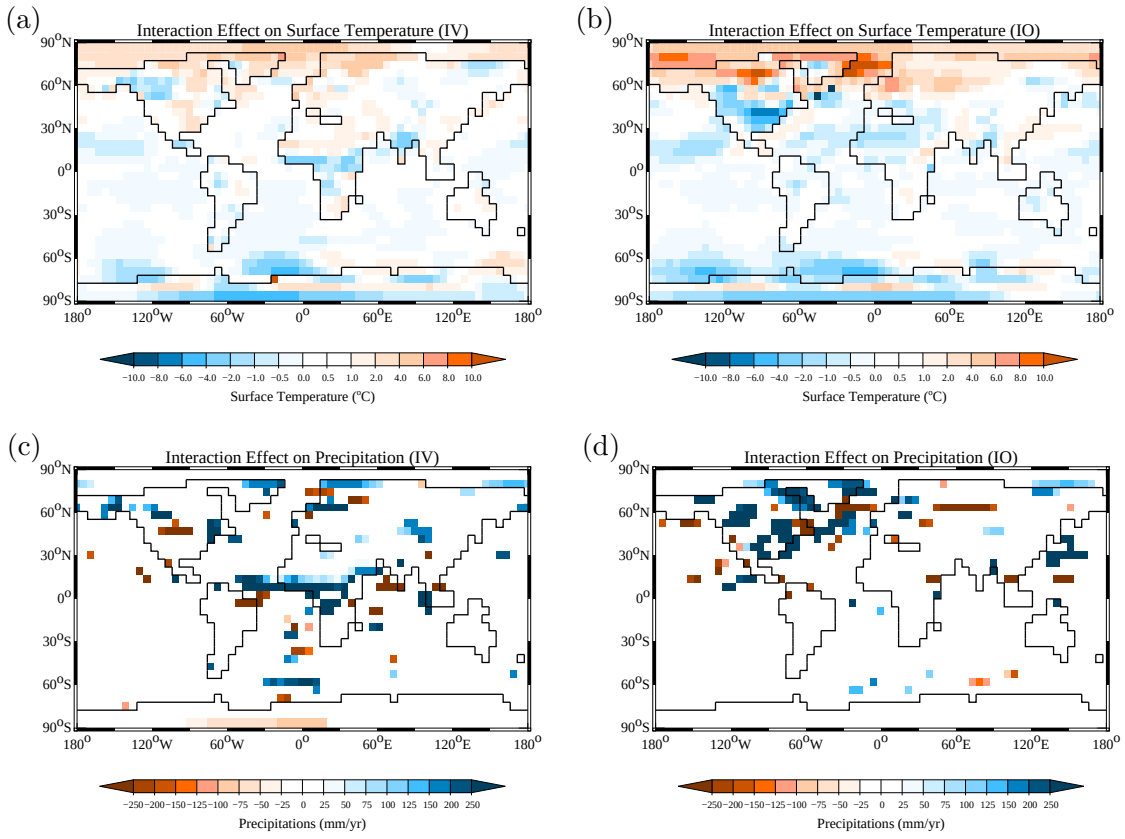

Fig. 11. Effects of **(a)** interaction IV on surface temperature; **(b)** interaction IO on surface temperature; **(c)** interaction IV on precipitations; **(d)** interaction IO on precipitations.

when adding the ice sheet and CO_2 effects together. Overall, our results fairly agree with results of Ganopolski (2003) and Jahn et al. (2005). Some differences may be attributed to the lack of oceanic circulation changes in our model, although differences in the magnitude of the results can also come from the different structures of the Planet Simulator and CLIMBER-2.

5.2 Focus on vegetation impact

The vegetation cover change produces a cooling of $-1.3°C$ in the experiment V. Its pure contribution is globally lower than the ice and CO_2 contributions. However, its local impacts are comparable and even larger than the local impacts of CO_2, especially on the continents and the northern latitudes of Eurasia, due to the taïga-tundra feedback (Ganopolski et al., 2001). The magnitude of the vegetation effect in our results, confirms once again the importance of the vegetation contribution to the LGM climate. The additional cooling induced by LGM vegetation cover can be seen in the difference between experiments LGM and CIO. This cools the climate by $-0.9°C$, which is in line with the cooling obtained by Ganopolski (2003) and Jahn et al. (2005) (respectively $-0.6°C$ and $-0.7°C$). It is also at the lower end (strongest cooling) of the range of temperature variations due to vegetation changes reported by Schneider von Deimling et al. (2006) ($-0.5°C$ to $-1°C$). The larger cooling in our results can therefore be attributed to a larger difference in the prescribed vegetation cover that nevertheless agrees well with the data. The additional vegetation impact in our results is also stronger than the impacts of prescribed vegetation reconstructions in previous studies (Crowley and Baum, 1997; Levis et al., 1999; Wyputta and McAveney, 2001). However, the weaker effects of vegetation in these studies could also be due to the use of fixed sea surface temperatures that leads to an underestimation of vegetation impacts, as shown by Ganopolski et al. (2001).

5.3 Ice and orography impacts

The separation of the ice cover and orography contributions shows that the ice albedo effect is the main contributor to the cooling of the Northern Hemisphere, whereas orography has only a local cooling impact over the ice sheet. Several studies have already investigated these two effects, but on the basis of a sequentially additive procedure (Rind, 1987;

Kageyama and Valdes, 2000). The isolation of both contributions allows us to attribute the atmospheric circulation changes in the Northern Hemisphere to the orography effect, but the strengthening of the westerlies of the Northern Hemisphere to the ice albedo effect. Similarly to Manabe and Broccoli (1985) and Broccoli and Manabe (1987a) we find that the presence of the Laurentide ice sheet has a predominant impact on the atmospheric circulation, causing a split flow of the westerlies into two branches that in turn leads to a disruption of the precipitation distributions in the Northern Hemisphere, and affects the surface temperature. We can also remark that the orographic contribution alone would have caused some warming in Europe and in the center of North America. This warming is more than compensated by the cooling effect of the ice cover. The resulting impact of the ice sheets (orography plus ice albedo) in these regions is weaker than the pure ice albedo effect.

5.4 Effects on precipitation

Nevertheless, the ice sheet impact is not limited to the climate in the Northern Hemisphere. The ice cover contribution significantly affects the tropical regions and is even the main contributor to tropical precipitation decrease over the continents and the oceans. Chiang et al. (2003), Chiang and Bitz (2005) and Broccoli et al. (2006) already related the reduction of convective activity and precipitation in the tropics and particularly the southwards shift of the ITCZ (Braconnot et al., 2000) to the presence of ice in the Northern Hemisphere. In our case, the pure contribution of the ice sheet cover is sufficient to produce a reduction of the sea surface temperature in the Northern Hemisphere as well as in the northern part of the tropics (more particularly in the equatorial Atlantic and Indian oceans). The meridional gradient across the equator is increased and the ITCZ shifted southwards. Interestingly, the addition of the orographic contribution intensifies the disruption of the tropical precipitation by warming the sea-surface temperature in the Southern Hemisphere.

The intense cooling of the continents in the Northern Hemisphere produced by the ice cover contribution and the persistance of snow also weakens the Asian summer monsoon, as in DeMenocal and Rind (1993). However, our results show an increase of precipitation over North East Asia that can be related to the strengthening of the Asian winter monsoon, as already obtained by Yanase and Abe Ouchi (2007) with simplified and coupled models of the PMIP2 simulations. The precipitation maximum during winter is also displaced to the Pacific, southwards of Southeast Asia. This can be linked to the southward shift of the westerly jet stream, as in Yanase and Abe Ouchi (2007).

Ice cover is not the only effect that leads to a disruption of tropical rainfall. The vegetation contribution also strongly affects the tropics. As noted by Kubatzki and Claussen (1998), the vegetation impacts remain essentially local, due partly to the use of fixed sea surface temperatures. However, the cooling produced over the continents of the Northern Hemisphere, mostly due to the albedo effect, is sufficient to reduce the convective activity of the ITCZ, as described in Crucifix and Hewitt (2005), and to shift the ITCZ southwards. Nevertheless the vegetation effect remains weaker than the ice albedo effect. Further, the addition of the vegetation contribution to the ice cover contribution reinforces the cooling and drying over the Northern Hemisphere, as well as the precipitation decrease over the ITCZ control location, even if the interactions of both factors tend to act in opposite directions. The vegetation contribution also warms and dries the tropical regions of South America and Africa, as mentioned by Levis et al. (1999). This effect is linked to the reduction of the tropical rainforest, decreasing the roughness length in the model that in turn reduces the surface evaporation.

For completeness, we should mention that neither the effects of lower CH_4 and N_2O concentrations in the atmosphere, nor those of the higher atmospheric dust content at the LGM have been taken into account in the present study. As mentioned in Sect. 3.1, their variations could lead to important additional cooling and provide feedbacks for the LGM climate system. Schneider von Deimling et al. (2006) notably show that the increase of atmospheric dustiness at the LGM yields a net global cooling of the same order of magnitude as the vegetation induced cooling.

5.5 Consistency with palaeo data

In order to estimate the consistency of the simulated LGM climate and of the boundary conditions impacts, we evaluated our results over Eurasia and Africa against the LGM climate reconstructed by Wu et al. (2007). We have restricted our comparison to the continental areas in order to limit the oceanic influence, since our model does not include an OGCM. The Wu et al. (2007) reconstruction was produced with an improved inverse vegetation model, using a recent version of BIOME4 (Kaplan, 2001) and pollen biome scores from the BIOME6000 project (Prentice and Jolly, 2000). Further, the improved inverse modelling method takes into account the direct physiological impact of the lower CO_2 concentration at LGM, reducing the bias in palaeoclimatic reconstruction (Ramstein et al., 2007).

We compare our model results to reconstructions by using zonal averages, following the approach of Kageyama et al. (2001). In order to keep the model averages comparable with the data coverage, we partitioned them into two sectors representing Western Europe and Africa 20° W−20° E) on one hand, and Eastern Europe, Eastern Africa and Western Siberia (20° E−60° E), on the other. The differentiation between two sectors allows us to clearly display the model results and the data with error bars, keeping the data points sufficiently well distributed in longitude over each one of the two sectors. It also allows us to highlight the meridional gradients in the studied climatic variables. Please notice

that the anomalies are calculated between a modern climate run (same conditions as for preindustrial, except for an atmospheric CO_2 concentration of 340 ppm) and the LGM run described above, in order to be compatible with the reconstructed anomalies. The averages are taken over land points only. Figures 12 and 13 show the zonal averages of the model anomalies and the data anomalies between LGM and modern climate for the mean temperature of the coldest month (MTCO), the mean temperature of the warmest month (MTWA), the mean annual temperature and precipitation (MAT and MAP, respectively). The data error bars are also shown, representing the 5–95% confidence interval for each reconstruction and the ± 2 standard deviation curves, representing the longitudinal dispersion of the model results.

The simulated MTCO anomalies are generally colder in Eurasia than in Africa, and colder over latitudes higher than 40° N, suggesting a stronger LGM meridional gradient, compared to present-day. The model tends to overestimate the cooling over Siberia in comparison with the data, but the results remain within the data error bars, which are quite large over this region (interval of possible values of the order of 25°C). The cooling over Northwestern Europe, linked to the presence of the Fennoscandian ice sheet, may also be overestimated, but no pollen data are available to confirm or contradict our results. The cooling is clearly underestimated over Africa. The model even gives a slight warming near the Equator.

The MTWA anomalies show a general cooling trend at the LGM, with some warming, especially over the eastern sector. The model reproduces quite well the absence of a net meridional gradient, but the variability of the model results is much stronger than the data error bars. This is due to the low resolution of the model and the average of the model results over large zones. The model tends to underestimate the cooling over Western Europe, but still produces a strong cooling over the ice sheet. The discrepancies are still present over Western Africa.

MAT values show a similar pattern to MTCO, even if the MAT anomalies are smaller than the MTCO ones. The model also simulates drier conditions than today, with a decrease of MAP that agrees with data. The model tends to overestimate the decrease in precipitation over high latitudes, but gives a slight increase of precipitation over the ice sheet. A strong decrease is produced in Equatorial Africa that is not reproduced in the data. However the MAP anomalies over Africa are generally in beter agreement with the data than the MAT anomalies, especially over the western sector.

Our results agree fairly well with the climatic reconstructions of Wu et al. (2007) over Europe and Western Siberia. They reproduce the south-west to north-east temperature gradient, with a decrease of MTCO cooling from Europe to Siberia, and the absence of significant MTWA gradient, as in the PMIP1 and PMIP2 model-pollen data comparisons carried out by Kageyama et al. (2001, 2006). Our results show a better agreement with the data, in particular over Western Europe, as we include the vegetation contribution, not taken into account in the PMIP1 simulations. Nevertheless, there are still regions where discrepancies remain significant. The model tends to overestimate the MTCO cooling and the dryness over Siberia, similar to several models in the PMIP1 project (Kageyama et al., 2001). As explained in Kageyama et al. (2001), it may also be due to the perturbation of atmospheric circulation produced by North Atlantic sea surface temperatures and sea-ice extent, computed by the slab ocean model. However, the MTCO cooling over Northwestern Europe is generally stronger than the ones produced by the models with computed sea surface temperatures used by Kageyama et al. (2001). Therefore, it is in better agreement with the data over this sector.

On the other hand, the MTWA cooling is underestimated over Western Europe (around 45° N), due to a decrease of MAP. These results may be related to too warm sea surface temperature computed by the slab model in the Mediterranean Sea, influencing the continental temperature and precipitation of this region and giving warmer and drier summers than in the reconstruction. The weakening of the westerlies due to orography changes (see Sect. 4.4) can also explain the warming of the region especially in summer. We cannot ascribe these discrepancies to the low resolution of the model or the poor representation of orography in this region. Jost et al. (2005) indeed find that these discrepancies persist at higher resolutions.

Over Eastern and South Africa, the model systematically underestimates the MTCO and MTWA cooling. This underestimation of the cooling by the model can be explained by the higher elevation of the data points (above 1500 m), in comparison to the model elevation (not exceeding 500 m). The reduction of the reconstructed temperature are then larger at higher elevation, as suggested by the reconstruction of temperature changes at the LGM from the snowline changes in East Africa carried out by Mark et al. (2005).

6 Conclusions

In this study, we used the Planet Simulator, an Earth System model of intermediate complexity to investigate the contributions of the ice sheet expansion and elevation, the lowering of the atmospheric CO_2 and of the vegetation cover change on the LGM climate. The vegetation distributions for the preindustrial and the LGM were obtained with the dynamic vegetation model CARAIB. They compare fairly well in terms of biomes with the results of the Palaeovegetation Mapping Project BIOME6000 (Prentice and Jolly, 2000).

We applied here the factor separation method of Stein and Alpert (1993), in order to rigorously determine the different contributions of the boundary condition modifications. The method also allowed us to isolate the pure contributions, as well as the interactions among the factors. This same method

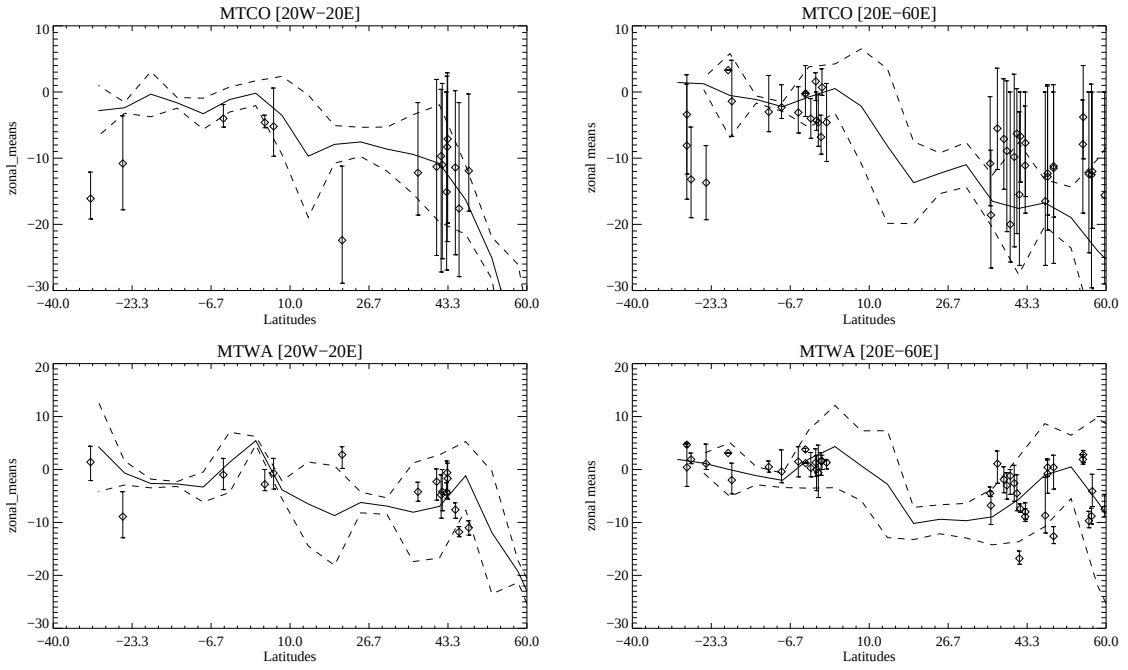

Fig. 12. Comparison between model results and data for the LGM-minus-PRESENT anomalies of the mean temperature of the coldest month (MTCO) and the mean temperature of the warmest month (MTWA), in the two sectors (20° W–20° E) and (20° E–60° E). For the model, the longitudinal averages over land points (solid lines) are shown with the ±2 standard deviation curves (dashed lines). Data points are represented by dots and shown with the 5–95% confidence intervals.

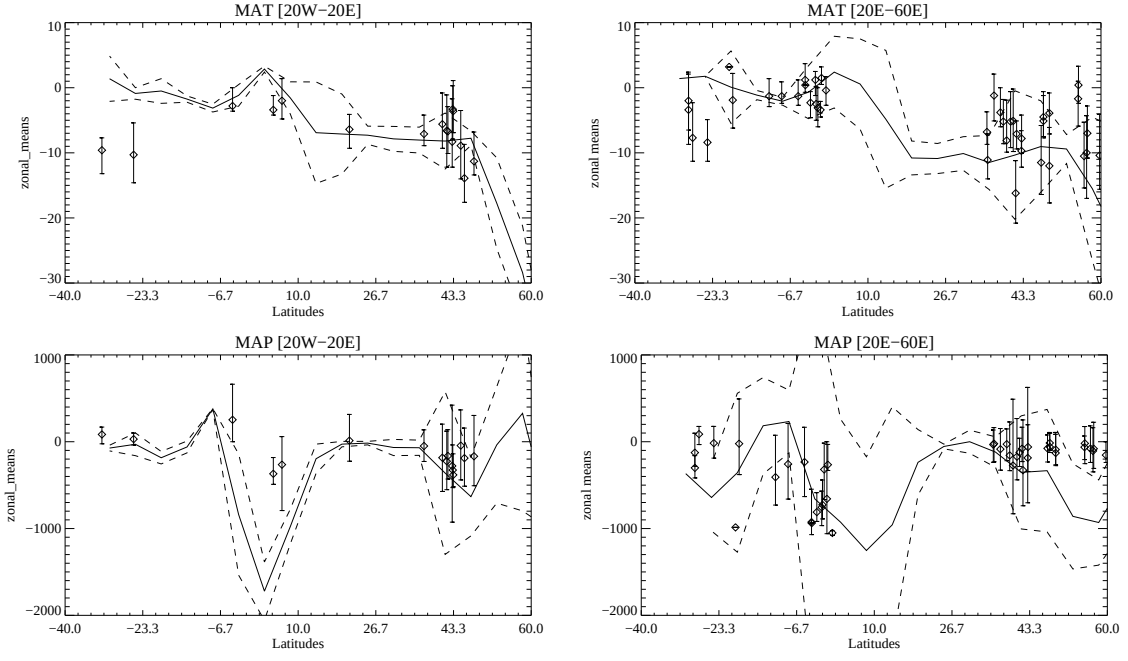

Fig. 13. Comparison between model results and data for the LGM-minus-PRESENT anomalies in the mean annual temperature (MAT) and the mean annual precipitation (MAP) — see Fig. 12 for more details.

was previously adopted in studies of Berger et al. (1996) and Jahn et al. (2005) e.g. who focused on a smaller set of factors.

Our results highlight once more the dominant cooling and drying effect of the ice sheet expansion on the global scale LGM climate. This finding confirms the conclusions of Ganopolski (2003) and Jahn et al. (2005). The next most important factors are the lower CO_2 concentration in the atmosphere and the vegetation cover change. Similarly to Broccoli and Manabe (1987b), we find that, locally, the ice albedo effect is also responsible for the strongest cooling in the Northern Hemisphere, while the reduction in atmospheric CO_2 is the main contributor to the Southern Hemisphere cooling. However, due to the lack of oceanic circulation changes in our model, we do not produce a strengthening of the northward heat transfer, as in Jahn et al. (2005). Therefore our results show a generally colder and dryer effect of the ice sheet in the Northern Hemisphere and a more homogeneous impact of the CO_2 reduction in comparison to Jahn et al. (2005).

The separation of the ice cover and orographic contributions shows that the ice albedo effect is the main contributor to the cooling of the Northern Hemisphere, whereas orography has only a local cooling impact over the ice sheet, and gives the weakest global impact on temperature of the series of pure contributions. Further, the ice cover expansion in the Northern Hemisphere is identified for being responsible for the tropical precipitation disruption and the southward shift of the ITCZ, as already mentioned in Chiang et al. (2003). The orographic changes at high latitudes mainly contribute to the disruption of the atmospheric circulation in the Northern Hemisphere, but do not have any significant impact in the tropics. According to Broccoli and Manabe (1987a), the presence of the Laurentide ice sheet has a predominant impact on the atmospheric circulation, causing a split flow of the westerlies into two branches, leading to a redistribution of the precipitation. This disruption of the precipitation causes some warming over the continents of the Northern Hemisphere and over the oceans. The cooling brought about by the ice cover, however, overcompensates for this warming.

In our experiments, the vegetation contribution induces strong cooling over the continents of the Northern Hemisphere, mainly caused by the increase of albedo, even comparable in magnitude to the ice cover and CO_2 induced cooling in some regions. Further, the vegetation effects are also sufficient to affect the tropical precipitation on land and on the oceans, causing a southward shift of the ITCZ, which is reinforced when we combine the ice and vegetation contributions. The additional effect of vegetation changes under LGM boundary conditions gives a global cooling in line with the results of Ganopolski (2003), Jahn et al. (2005) and Schneider von Deimling et al. (2006), but slightly stronger due to the more contrasting vegetation reconstruction prescribed here.

The combinations of the factors generate many interactions, globally opposed to the pure contributions and weaker. However, locally the interaction effects are more complex and may either reinforce or weaken the pure contributions, depending on the regions of the globe and on the climatic mechanism involved.

Finally, our LGM climate results agree fairly well with the climatic reconstructions of Wu et al. (2007) over Europe and Western Siberia, notably due to the inclusion of vegetation changes. Our results reproduce well the south-west to north-east MTCO gradient from Europe to Siberia, and the absence of significant MTWA gradient, as in the PMIP1 and PMIP2 model-pollen data comparisons carried out by Kageyama et al. (2001, 2006). However, our results do not support the strong cooling over Africa that are due to the use of elevated data points for the paleoclimatic reconstructions.

Acknowledgements. We thank Michel Crucifix for helpful discussions and for pointing out the Stein and Alpert (1993) method to us. We acknowledge the efforts of the Planet Simulator team (especially Klaus Fraedrich, Edilbert Kirk and Frank Lunkeit) for making available their model as Open Source Software and for the sustained development and help. We thank Stefan Lorenz for providing the ECHAM4 data. Comments by Andrey Ganopolski and one anonymous reviewer helped to improve the manuscript submitted for discussion. A.-J. Henrot is a Research Fellow and G. Munhoven a Research Associate with the Belgian Fund for Scientific Research (F.R.S.-FNRS). Support for the work of S. Brewer was provided by FRFC convention no. 2.4555.06.

Edited by: M. Claussen

References

Adams, J. M., Faure, H., Faure-Denard, L., McGlade, J. M., and Woodward, F. I.: Increases in the terrestrial carbon storage from the Last Glacial Maximum to the present, Nature, 348, 711–714, 1990.

AMIP2: The second phase of the Atmospheric Model Intercomparison Project (AMIP2), Workshop WCRP/WGNE, Météo France, Toulouse, France, 2004.

Berger, A., Dutrieux, A., Loutre, M., and Tricot, C.: Paleoclimate sensitivity to CO_2 and insolation, Scientific Report 6, Institut d'Astronomie et de Géophysique Georges Lemaitre, Louvain-la-Neuve, Belgium, 1996.

Bigelow, N. H., Brubaker, L. B., Edwards, M. E., Harrison, S. P., Prentice, I. C., Anderson, P. M., Andreev, A. A., Bartlein, P. J., Christensen, T. R., Cramer, W., Kaplan, J. O., Lozhkin, A. V., Matveyeva, N. V., Murray, D. V., McGuire, A. D., Razzhivin, V. Y., Ritchie, J. C., Smith, B., Walker, D. A., Gajewski, K., Wolf, V., Holmqvist, B. H., Igarashi, Y., Kremenetskii, K., Paus, A., Pisaric, M. F. J., and Vokova, V. S.: Climate change and Arctic ecosystems I. Vegetation changes north of 55° N between the last glacial maximum, mid-Holocene and present, J. Geophys. Res., 108, 8170, doi:10.1029/2002JD002558, 2003.

Braconnot, P., de Noblet, S. J. N., and Ramstein, G.: Mid-Holocene and Last Glacial Maximum African monsoon changes as simulated within the Paleoclimate Modelling Intercomparison Project, Global Planet. Change, 26, 51–66, 2000.

Braconnot, P., Otto-Bliesner, B., Harrison, S., Joussaume, S., Peterchmitt, J.-Y., Abe-Ouchi, A., Crucifix, M., Driesschaert, E., Fichefet, Th., Hewitt, C. D., Kageyama, M., Kitoh, A., Laîné, A., Loutre, M.-F., Marti, O., Merkel, U., Ramstein, G., Valdes, P., Weber, S. L., Yu, Y., and Zhao, Y.: Results of PMIP2 coupled simulations of the Mid-Holocene and Last Glacial Maximum – Part 1: experiments and large-scale features, Clim. Past, 3, 261–277, 2007, http://www.clim-past.net/3/261/2007/.

Broccoli, A. J. and Manabe, S.: The effects of the Laurentide ice sheet on north american climate during the last glacial maximum, Géographie physique et Quaternaire, 41, 291–299, 1987a.

Broccoli, A. J. and Manabe, S.: The influence of continental ice, atmospheric CO_2, and land albedo on the climate of the last glacial maximum, Climate Dyn., 1, 87–99, 1987b.

Broccoli, A. J., Dahl, K. A., and Stouffer, R. J.: The response of the ITCZ to Northern Hemisphere cooling, Geophys. Res. Lett., 33, L01702, doi:10.1029/2005GL024546, 2006.

Cheddadi, R., Vendramin, G., Litt, T., François, L., Kageyama, M., Lorentz, S., Laurent, J., de Beaulieu, J., Sadori, L., Jost, A., and Lunt, D.: Imprints of glacial refugia in the modern genetic diversity of Pinus sylvestris, Global Ecol. Biogeogr., 15, 271–282, 2006.

Chiang, J. C. H. and Bitz, C. M.: Influence of high latitude ice cover on the marine Intertropical Convergence Zone, Climate Dyn., 25, 477–496, 2005.

Chiang, J. C. H., Biasutti, M., and Battisti, D. S.: Sensitivity of the Atlantic Intertropical Convergence Zone to Last Glacial Maximum boundary conditions, Paleoceanography, 18, 1094, doi:10.1029/2003PA000916, 2003.

CLIMAP Project Members: The Surface of the Ice-Age Earth, Science, 191, 1131–1137, 1976.

Crowley, T. J. and Baum, S. K.: Effect of vegetation on an ice-age climate model simulation, J. Geophys. Res., 102, 16463–16480, 1997.

Crucifix, M. and Hewitt, C. D.: Impact of vegetation changes on the dynamics of the atmosphere at the Last Glacial Maximum, Climate Dyn., 25, 447–459, 2005.

DeMenocal, P. B. and Rind, D.: Sensitivity of Asian and African Climate to Variations in Seasonal Insolation, Glacial Ice Cover, Sea Surface Temperature, and Asian Orography, J. Geophys. Res., 98, 7265–7287, 1993.

Fraedrich, K., Kirk, E., and Lunkeit, F.: PUMA Portable University Model of the Atmosphere, Tech. Rep. 16, Meteorologisches Institut, Universität Hamburg, Hamburg, http://www.mad.zmaw.de/fileadmin/extern/documents/reports/ReportNo.16.pdf, 1998.

Fraedrich, K., Jansen, H., Kirk, E., Luksch, U., and Lunkeit, F.: The Planet Simulator: Towards a user friendly model, Meteorol. Z., 14, 299–304, doi:10.1127/0941-2948/2005/0043, 2005.

Fraedrich, K., Jansen, H., Kirk, E., and Lunkeit, F.: The Planet Simulator : Green planet and desert world, Meteorol. Z., 14, 305–314, doi:10.1127/0941-2948/2005/0044, 2005b.

François, L., Lorenz, S., Ghislain, M., Cheddadi, R., and Jolly, D.: Impact of reduced tropical sea surface temperatures on the reconstruction of climate and land vegetation at the last glacial maximum, in: Proceedings XVI INQUA Congress, p. 130, 2003.

François, L. M., Delire, C., Warnant, P., and Munhoven, G.: Modelling the Glacial-Interglacial Changes in the Continental Biosphere, Global Planet. Change, 16–17, 37–52, doi:10.1016/S0921-8181(98)00005-8, 1998.

François, L. M., Goddéris, Y., Warnant, P., Ramstein, G., de Noblet, N., and Lorenz, S.: Carbon stocks and isotopic budgets of the terrestrial biosphere at mid-Holocene and last glacial maximum times, Chem. Geol., 159, 163–189, doi:10.1016/S0009-2541(99)00039-X, 1999.

Galy, V., François, L., France-Lanord, C., Faure, P., Kudrass, H., Palhol, F., and Singh, S. K.: C4 plants decline in the Himalayan basin since the Last Glacial Maximum, Quaternary Sci. Rev., 27, 1396–1409, 2008.

Ganopolski, A.: Glacial integrative modelling, Phil. Trans. R. Soc. Lond. Ser. A, 361, 1871–1884, 2003.

Ganopolski, A. and Rahmstorf, S.: Rapid changes of glacial climate simulated in a coupled climate model, Nature, 409, 153–158, 2001.

Ganopolski, A., Petoukhov, V., Rahmstorf, S., Brovkin, V., Claussen, M., Eliseev, A., and Kubatzki, C.: CLIMBER-2: a climate system model of intermediate complexity. II. Model sensitivity, Climate Dyn., 17, 735–751, 2001.

Harrison, S. P., Yu, P., Takahara, H., and Prentice, I. C.: Paleovegetation – Diversity of temperate plants in east Asia, Nature, 413, 129–130, 2001.

Hewitt, C., Stouffer, R., Broccoli, A., Mitchell, J., and Valdes, P.: The effect of ocean dynamics in a coupled GCM simulation of the Last Glacial Maximum, Climate Dyn., 20, 203–218, 2003.

Hewitt, C. D. and Mitchell, J. F. B.: Radiative forcing and response of a GCM to ice age boundary conditions: cloud feedback and climate sensitivity, Climate Dyn., 13, 821–834, 1997.

Jahn, A., Claussen, M., Ganopolski, A., and Brovkin, V.: Quantifying the effect of vegetation dynamics on the climate of the Last Glacial Maximum, Clim. Past, 1, 1–7, 2005, http://www.clim-past.net/1/1/2005/.

Jost, A., Lunt, D., Kageyama, M., Abe-Ouchi, A., Peyron, O., Valdes, P. J., and Ramstein, G.: High-resolution simulations of the last glacial maximum climate over Europe: a solution to discrepancies with continental palaeoclimatic reconstructions?, Climate Dyn., 24, 577–590, 2005.

Joussaume, S. and Taylor, K.: The Paleoclimate Modeling Intercomparison Project, in: Paleoclimate Modeling Intercomparison Project (PMIP), edited by Braconnot, P., no. 1007 in WMO/TD, 9–24, WMO, Geneva (CH), (WCRP-111), 2000.

Kageyama, M. and Valdes, P. J.: Impacts of the North American ice-sheet orography on the Last Glacial Maximum eddies and snowfall, Geophys. Res. Lett., 27, 1515–1518, 2000.

Kageyama, M., Peyron, O., Pinot, S., Tarasov, P., Guiot, J., Joussaume, S., and Ramstein, G.: The Last Glacial Maximum climate over Europe and western Siberia: a PMIP comparison between models and data, Climate Dyn., 17, 23–43, 2001.

Kageyama, M., Lané, A., Abe-Ouchi, A., Braconnot, P., Cortijo, E., Crucifix, M., Vernal, A. D., Guiot, J., Hewitt, C. D., Kitoh, A., Marti, M. K. O., Ohgaito, R., Otto-Bliesner, B., Peltier, W. R., Rosell-Melé, A., Vettoretti, G., Weber, S. L., Yu, Y., and MARGO Project Members: Last Glacial Maximum temperatures over the North Atlantic, Europe and western Siberia: a comparison between PMIP models, MARGO sea-surface temperatures and pollen-based reconstructions, Quaternary Sci. Rev., 25, 2082–2102, 2006.

Kaplan, J. O.: Geophysical application of vegetation modeling, PhD Thesis, Lund University, Lund, 2001.

Kim, S.-J., Flato, G., and Boer, G.: A coupled climate model simulation of the Last Glacial Maximum, Part 2: approach to equilibrium, Climate Dyn., 20, 635–661, 2003.

Kubatzki, C. and Claussen, M.: Simulation of the global biogeophysical interactions during the Last Glacial Maximum, Climate Dyn., 14, 461–471, 1998.

Kucera, M., Rosell-Melé, A., Schneider, R., Waelbroeck, C., and Weinelt, M.: Multiproxy approach for the reconstruction of the glacial ocean surface (MARGO), Quaternary Sci. Rev., 24, 813–819, 2005.

Laurent, J.-M., François, L., Bar-Hen, A., Bel, L., and Cheddadi, R.: European Bioclimatic Affinity Groups: data-model comparisons, Global Planet. Change, 61, 28–40, 2008.

Levis, S., Foley, J. A., and Pollard, D.: CO_2, climate and vegetation feedbacks at the Last Glacial Maximum, J. Geophys. Res., 104, 31191–31198, 1999.

Lynch-Stieglitz, J., Adkins, J., Curry, W., Dokken, T., Hall, I., Herguera, J., Hirschi, J.-M., Ivanova, E., Kissel, C., Marchal, O., Marchitto, T., McCave, I., McManus, J., Mulitza, S., Ninnemann, U., Peeters, F., Yu, E.-F., and Zahn, R.: Atlantic Meridional Overturning Circulation during the Last Glacial Maximum, Science, 316, 66–69, 2007.

Manabe, S. and Broccoli, A. J.: The influence of Continental Ice Sheets on the Climate of an Ice Age, J. Geophys. Res., 90, 2167–2190, 1985.

Mark, B., Harrison, S., Spessa, A., New, M., Evans, D., and Helmens, K.: Tropical snowline changes at the Last Glacial Maximum: A global assessment, Quatern. Int., 138–139, 168–201, 2005.

Nemry, B., François, L. M., Warnant, P., Robinet, F., and Gérard, J.-C.: The seasonality of the CO_2 exchange between the atmosphere and the land biosphere: A study with a global mechanistic vegetation model, J. Geophys. Res., 101, 7111–7125, 1996.

Otto, D., Rasse, D., Kaplan, J., Warnant, P., and François, L.: Biospheric carbon stocks reconstructed at the Last Glacial Maximum: comparison between general circulation models using prescribed and computed sea surface temperatures, Global Planet. Change, 33, 117–138, 2002.

Pedersen, T. F., François, R., François, L., Alverson, K., and McManus, J.: The Late Quaternary History of Biogeochemical Cycling of Carbon, in: Paleoclimate, Global Change and the Future, edited by: Alverson, K. D., Bradley, R. S., and Pedersen, T. F., Springer-Verlag, Berlin, Germany, Chap. 4, 63–78, 2003.

Peltier, W. R.: Global glacial isostasy and the surface of the ice-age Earth: the ICE-5G (VM2) Model and GRACE, Annu. Rev. Earth Planet. Sci., 32, 49–111, 2004.

Petit, J.-R., Jouzel, J., Raynaud, D., Barkov, N. I., Barnola, J.-M., Basile, I., Bender, M., Chappellaz, J., Davis, M., Delaygue, G., Delmotte, M., Kotlyakov, V. M., Legrand, M., Lipenkov, V. Y., Lorius, C., Pépin, L., Ritz, C., Saltzman, E., and Stievenard, M.: Climate and atmospheric history of the past 420,000 years from the Vostok ice core, Antarctica, Nature, 399, 429–436, 1999.

Petoukhov, V., Ganopolski, A., Brovkin, V., Claussen, M., Eliseev, A., Kubatzki, C., and Rahmstorf, S.: CLIMBER-2: a climate system model of intermediate complexity. Part I: model description and performance for present climate, Climate Dyn., 16, 1–17, 2000.

Pickett, E., Harrison, S. P., Hope, G., Harle, K., Dodson, J. R., Kershaw, A. P., Prentice, I. C., Backhouse, J., Colhoun, E. A., D'Costa, D., Flenley, J., Grindrod, J., Haberle, S., Hassell, C., Kenyon, C., Macphail, M., Martin, H., Martin, A. H., McKenzie, M., Newsome, J. C., Penny, D., Powell, J., Raine, I., Southern, W., Sutra, J., Thomas, I., van der Kaars, S., and Ward, J.: Pollen-based reconstructions of biome distributions for Australia, South East Asia and the Pacific (SEAPAC region) at 0, 6000 and 18,000 14C yr B.P., J. Biogeogr., 31, 1381–1444, 2004.

Prentice, I. C., Jolly, D., and BIOME 6000 Participants: Mid-Holocene and glacial-maximum vegetation geography of the northern continents and Africa, J. Biogeogr., 27(3), 507–519, 2000.

Ramstein, G., Kageyama, M., Guiot, J., Wu, H., Hély, C., Krinner, G., and Brewer, S.: How cold was Europe at the Last Glacial Maximum? A synthesis of the progress achieved since the first PMIP model-data comparison, Clim. Past, 3, 331–339, 2007, http://www.clim-past.net/3/331/2007/.

Rind, D.: Components of the Ice Age Circulation, J. Geophys. Res., 92, 4241–4281, 1987.

Roeckner, E., Arpe, K., Bengtsson, L., Christoph, M., Claussen, M., Dumenil, L., Esch, M., Giorgetta, M., and Schlese, U.: The Atmospheric General Circulation Model ECHAM4: model description and simulation of present day climate, Tech. Rep. 218, Max-Planck-Institute for Meteorology, Hamburg, 1996.

Schneider von Deimling, T., Ganopolski, A., and Held, H.: How cold was the Last Glacial Maximum?, Geophys. Res. Lett., 33, L14709, doi:10.1029/2006GL026484, 2006.

Stein, U. and Alpert, P.: Factor Separation in Numerical Simulations, J. Atmos. Sci., 50(14), 2107–2115, 1993.

Warnant, P., François, L. M., Strivay, D., and Gérard, J.-C.: CARAIB: A global model of terrestrial biological productivity, Global Biogeochem. Cy., 8, 255–270, 1994.

Weber, S. L., Drijfhout, S. S., Abe-Ouchi, A., Crucifix, M., Eby, M., Ganopolski, A., Murakami, S., Otto-Bliesner, B., and Peltier, W. R.: The modern and glacial overturning circulation in the Atlantic ocean in PMIP coupled model simulations, Clim. Past, 3, 51–64, 2007, http://www.clim-past.net/3/51/2007/.

Williams, J. W., Webb III, T., Richard, P. H., and Newby, P.: Late Quaternary biomes of Canada and the eastern United States, J. Biogeogr., 27, 585–607, 2000.

Wu, H., Guiot, J., Brewer, S., and Guo, Z.: Climatic changes in Eurasia and Africa at the last glacial maximum and mid-Holocene: reconstruction from pollen data using inverse vegetation modelling, Climate Dyn., 29, 211–229, 2007.

Wyputta, U. and McAveney, B. J.: Influence of vegetation changes during the Last Glacial Maximum using the BMRC atmospheric general circulation model, Climate Dyn., 17, 923–932, 2001.

Yanase, W. and Abe-Ouchi, A.: The LGM surface climate and atmospheric circulation over East Asia and the North Pacific in the PMIP2 coupled model simulations, Clim. Past, 3, 439–451, 2007, http://www.clim-past.net/3/439/2007/.